the X-ray structural data where the metal ligand bond lengths in the tris complex are about 10% longer than those in the bis complexes.

A summary of the metal–ligand vibrations assigned in this report is given in Table V, which clearly shows a general correlation between the mass of the metal atom and the frequency difference between the symmetric and antisymmetric metal–ligand modes. The frequencies of the antisymmetric modes are higher than the corresponding symmetric modes with Cu(II), almost equal with Pd(II), and lower with Pt(II) complexes.

Conclusions

This investigation illustrates the application of the technique of using the metal-isotope natural abundances,[21] in conjunction with other methods in the assignment of the far-infrared spectra, by providing a means of identifying the nickel–sulfur stretch in $Ni(Htsc)_2Cl_2$, together with an explanation for its exceptionally high deuteration shift and also by confirming the assignment of the metal–sulfur stretching modes in $Cu(Htsc)_2Cl$ and $Ni(tsc)_2$. The higher frequency assigned for the Ni–S stretching mode compares favorably with assignments for similar complexes in the literature.[22,24]

A comparison of the observed metal-isotope natural abundance splittings with that calculated from a highly simplified linear triatomic sulfur–metal–sulfur model is illustrated graphically in Figure 9. The good agreement shown suggests the presence of relatively pure metal-sulfur stretching modes in these complexes except in the case of $Ni(Htsc)_2Cl_2$-d_{10}, which shows an exceptional deviation arising from vibrational coupling with other modes.

Clearly, this technique of using the metal-isotope natural abundance has its greatest value in cases where the more elegant matrix-isolation technique is inapplicable due to experimental difficulties like insufficient volatility and solubility.

This investigation stresses the need for a reliable assignment before embarking on an approximate normal-coordinate analysis of complex vibrational systems. The relatively new IINS spectroscopy becomes a very powerful tool when used together with the other vibrational spectroscopic techniques in the vibrational analysis of complicated systems. It would be relevant at this point to note the elegance of IINS spectroscopy in the identification of the normal modes involving hydrogen movement in complex systems without depending on the success of deuterium substitution studies with their inherent complications due to the possible changes in the vibrational mode mixing.

Acknowledgment. Assistance given by the University support group headed by D. H. C. Harris at AERE, Harwell, is gratefully acknowledged.

Registry No. $Cu(Htsc)_2Cl_2$, 37981-04-7; $Cu(Htsc)_2Br_2$, 80228-80-4; $Ni(Htsc)_2Cl_2$, 21360-11-2; $Ni(Htsc)_2Br_2$, 53277-11-5; $Ni(tsc)_2$, 21360-12-3; $Ni(Htsc)_3Cl_2$, 36252-57-0; $Pd(Htsc)_2Cl_2$, 21360-15-6; $Pd(Htsc)_2Br_2$, 59532-29-5; $Pd(Htsc)_2I_2$, 59532-30-8; $Pd(tsc)_2$, 21360-16-7; $Pt(Htsc)_2Cl_2$, 21360-18-9; $Pt(Htsc)_2Br_2$, 59598-81-1; $Pt(Htsc)_2I_2$, 59685-11-9; $Ni(Htsc)_3Br_2$, 36252-58-1.

(24) See, for example: Siiman, O.; Fresco, J. *Inorg. Chem.* **1969**, *8*, 1846. Schlapfer, C. W; Nakamoto, K. *Inorg. Chim. Acta* **1972**, *6(1)*, 177.
(25) Gamlen, P. H; Hall, N. F; Taylor, A. D. Report RRL 74/693, AERE, Harwell, 1974.
(26) Willis, B. T. M., Ed. "Chemical Applications of Thermal Neutron Scattering"; Oxford University Press: London, 1973.

Contribution from the Laboratoire de Chimie Physique Organique, ERA CNRS 222, Université de Nancy I, 54037 Nancy Cedex, France

Structure and Dynamics of Complexes of the Uranyl Ion with Nonamethylimidodiphosphoramide (NIPA). 2. NMR Studies of Complexes $[UO_2(NIPA)_2X](ClO_4)_2$ with X = H_2O, MeOH, EtOH, or Me_2CO

L. RODEHÜSER, P. R. RUBINI, K. BOKOLO, and J.-J. DELPUECH*

Received March 16, 1981

The ^{31}P and ^1H spectra at −90 °C of the title uranyl complex ions (prepared as solutions of the solid perchlorates in inert anhydrous organic solvents (CH_3NO_2, CH_2Cl_2)) reveal a pentacoordinated arrangement of two symmetrically doubly bonded NIPA molecules and one solvent molecule about the uranyl group. In the case of $[UO_2(NIPA)_2(EtOH)](ClO_4)_2$, an intermolecular exchange between bound and free ethanol molecules is observed above −75 °C upon addition of ethanol to a solution of the complex. The observed rate law, $k_{inter} = kK[EtOH]/(1 + K[EtOH])$ is accounted for by the existence of an outer-sphere complex $[UO_2^{2+}(NIPA)_2(EtOH)]EtOH$ in fast equilibrium (K) with the initial complex and free ethanol. The rate-determining step (k) consists of an outer-sphere to inner-sphere interchange of ethanol molecules. The thermodynamic and kinetic parameters are K(25 °C) = 15.8 dm^3 mol^{-1}, k(25 °C) = 1.0×10^4 s^{-1}, ΔH and $\Delta H_{inter}^{\ddagger}$ = −4.8 and 7.6 kcal mol^{-1}, and ΔS and $\Delta S_{inter}^{\ddagger}$ = −10.7 and −14.7 eu. A second exchange takes place at higher temperatures (above −30 °C) yielding full dynamic equivalence of the phosphorus nuclei of the coordinated NIPA molecules. The observed rate law $k_{intra} = k_{ex}/(1 + K[EtOH])$ reveals that the internal rearrangement of NIPA molecules occurs on the complex ion $[UO_2(NIPA)_2(EtOH)]^{2+}$ but not on the outer-sphere complex: k_{ex}(25 °C) = 0.91×10^3 s^{-1}, $\Delta H_{intra}^{\ddagger}$ = 10.6 kcal mol^{-1}, and $\Delta S_{intra}^{\ddagger}$ = −9.4 eu. Possible mechanisms for this exchange are discussed.

Introduction

In an earlier publication[1] we described the structure of a uranyl complex with the diphosphorylated bidentate ligand nonamethylimidodiphosphoramide (NIPA) = $(NMe_2)_2P(O)NMeP(O)(NMe_2)_2$), a powerful neutral chelating reagent.[2] Standard procedures[3-5] to synthesize NIPA complexes use hydrated metallic perchlorates, which are dissolved in a mixture of ethanol and ethyl orthoformate so as to obtain anhydrous solutions of the metallic perchlorates. The chelating

(1) Part 1: Bokolo, K.; Delpuech, J.-J.; Rodehüser, L.; Rubini, P. R. *Inorg. Chem.* **1981**, *20*, 992.
(2) Rubini, P. R.; Rodehüser, L.; Delpuech, J.-J. *Inorg. Chem.* **1979**, *18*, 2962.
(3) De Bolster, M. W. G.; Groeneveld, W. L. *Recl. Trav. Chim. Pays-Bas* **1972**, *91*, 171.
(4) Van Leeuwen, P. W. N. M.; Groeneveld, W. L. *Inorg. Nucl. Chem. Lett.* **1967**, *3*, 145.
(5) Karayannis, N. M.; Bradshaw, E. E.; Pytlewski, L. L.; Labes, N. M. *J. Inorg. Nucl. Chem.* **1970**, *32*, 1079.

0020-1669/82/1321-1061$01.25/0

reagent is added to the above solutions, and the complexes precipitate on addition of anhydrous ether (cf. Experimental Section). Applied to the case of uranyl perchlorate, however, this procedure resulted in complex solutions of three uranyl species depending on the overall [NIPA]:[UO_2^{2+}] molar ratio: $UO_2(NIPA)_3(ClO_4)_2$, which was described in part 1,[1] a binuclear dimeric cation $[(UO_2)_2(NIPA)_5]^{4+}$,[35] and $[UO_2(NIPA)_2EtOH](ClO_4)_2$ (**3**). The last one can be isolated in ethanol solution with a [NIPA]:[UO_2^{2+}] ratio close to 2 (see Experimental Section). We obtained also the complexes $[UO_2(NIPA)_2X](ClO_4)_2$ with X = H_2O (**1**), MeOH (**2**), and Me_2CO (**4**) when water, methanol, or acetone were used as solvent. These complexes are soluble and stable in a 2:1 (v/v) mixture of dichloromethane and nitromethane ("C_2N"), even in the presence of an additional amount of ligand X. The influence of added ligand X upon the rates of intramolecular and intermolecular ligand exchanges is studied in the case of complex (**3**). Ligand substitution in mixed uranyl solvates is not well documented in the literature and may play an important role in the extraction of uranyl salts from aqueous solutions.

Experimental Section

Materials. Nonamethylimidodiphosphoramide was synthesized following a procedure described elsewhere.[1,6,7] The solvents used in the experiments were distilled Fluka "puriss" grade nitromethane, Prolabo "normapur" grade dichloromethane, Merck "absolute" ethanol, methanol dehydrated by reaction with magnesium methoxide, and SDS "puran" grade acetone. All solvents were kept for further dehydration over molecular sieves (4 Å) in the dark. Anhydrous diethyl ether (Baker "analyzed") was used for synthesis. The various complexes were prepared in the following way starting from $UO_2(ClO_4)_2 \cdot xH_2O$, with $x \approx 6$ (Alfa Ventron).

(a) $[UO_2(NIPA)_2(EtOH)](ClO_4)_2$. A 0.05-mol sample of the hydrated uranyl perchlorate was dissolved in 10 cm^3 of ethyl orthoformate and 5 cm^3 of anhydrous ethanol and stirred for some hours. Upon addition of 0.11 mol of NIPA dissolved in 5 cm^3 of ethanol, the complex precipitated immediately. It was collected by filtration, washed several times with anhydrous ether, and dried under reduced pressure. Recrystallization of the raw complex from ethanol yielded the salt in the form of yellow needles. Anal. Calcd for $[UO_2(NIPA)_2(EtOH)](ClO_4)_2$: C, 21.57; H, 5.43; N, 12.58; Cl, 6.37; P, 11.13; U, 21.38. Found: C, 21.61; H, 5.29; N, 12.24; Cl, 5.62; P, 11.07; U, 21.32.

(b) $[UO_2(NIPA)_2(MeOH)](ClO_4)_2$. The same procedure was used as described for **3**, replacing the ethyl orthoformate and ethanol by methyl orthoformate and methanol.

(c) $[UO_2(NIPA)_2(Me_2CO)](ClO_4)_2$. A 0.05-mol sample of hydrated uranyl perchlorate was dissolved in 15 cm^3 of dry acetone. For dehydration of the salt, ca. 5 g of freshly activated molecular sieves (3 Å) were added to the solution. After addition of 0.1 mol of NIPA in 5 cm^3 of acetone, the solution was stirred for 1 h. The molecular sieves were removed by filtration, and the solution was allowed to stand overnight. The complex precipitated slowly in the form of yellow crystals.

(d) $[UO_2(NIPA)_2(H_2O)](ClO_4)_2$ is formed on addition of an excess of NIPA to an aqueous solution of uranyl perchlorate, the complex being but sparingly soluble in water.

All solutions were prepared by weight. All preparations were carried out in a glovebox under purified argon.

NMR Spectroscopy. The equipment for the registration and treatment of the NMR spectra was the same as that described in part 1.

Line-Shape Measurements. Two types of ligand exchange (intra- and intermolecular) were examined on 0.099 M solutions of complex **3**, the first one in the temperature range from −30 to +20 °C and the second one from −75 to −45 °C. "Static spectra", i.e., reference

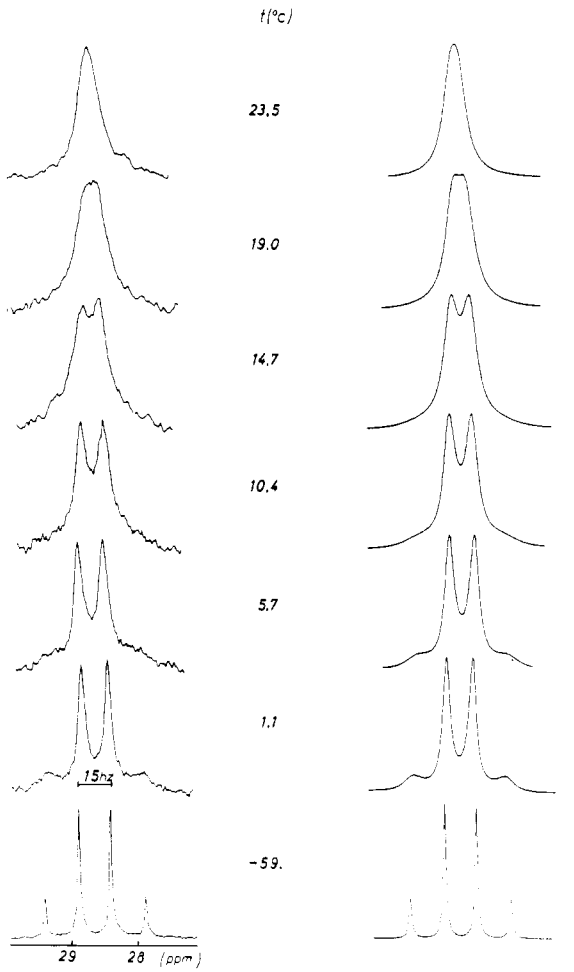

Figure 1. Experimental and calculated best fit $^{31}P\{^1H\}$ (32.44 MHz) line shapes (on the left- and right-hand sides of the figure) of a $[UO_2(NIPA)_2EtOH]^{2+}$ (0.099 M) + ethanol (1.016 M) solution in a 2:1 v/v CH_2Cl_2/CD_3NO_2 mixture, at temperatures of 23.5, 19.0, 14.7, 10.4, 5.7, 1.1, and −59 °C (from top to bottom). Best fit values k_{intra} = 105, 78, 54, 38, 26, 18, 0 s^{-1}, respectively.

spectra without any line broadening due to exchange phenomena, were obtained at −90 °C. Both types of exchange depended upon the amount of added extra ethanol, and several concentrations of added ethanol were used for these experiments. The *intramolecular* exchange is accompanied by a ^{31}P site exchange of the type AB ⇄ BA (Figure 1). Theoretical line shapes were computed from a density matrix formalism[8] and program EXCH14.[9] NMR rate constants k_{intra} were adjusted by trial and error so as to obtain the best fit of the theoretical curves to the experimental results (Figure 1). The *intermolecular* exchange is followed by observing the methyl ^1H signals of bound ethanol (lines 1–3) and free ethanol (lines 4–6) in the order of increasing field strength (Figure 2). The intensity ratios are equal to r = [salt]:[added "free" ethanol]. The intermolecular exchange of ethanol molecules is accompanied by a ^1H site exchange between lines 1 and 4, 2 and 5, and 3 and 6, respectively, with a common NMR rate constant k_{inter} for the overall process bound ethanol $\underset{k_{inter}}{\rightleftharpoons}$ free ethanol. Theoretical line shapes are computed from a matrix formalism due to Anderson,[10] Kubo,[11] and Sack[12] and the program ECHGN[13] (Figure 2). The population vector **P** and the exchange matrix **E** are

$$\mathbf{P} = |r,\ 2r,\ r,\ 1,\ 2,\ 1|$$

(6) (a) Lester, P. *Chem. Abstr.* **1955**, *49*, 6300g. (b) Pianka, M.; Owen, B. D. *J. Appl. Chem.* **1955**, *5*, 525. (c) Arceneaux, R. L.; Frick, J. G.; Leonard, E. K.; Reid, J. D. *J. Org. Chem.* **1959**, *24*, 1419. (d) Debo, A. *Chem. Abstr.* **1960**, *54*, 24397e.
(7) De Bolster, M. W. G.; Groeneveld, M. W. *Recl. Trav. Chim. Pays-Bas* **1971**, *90*, 687.
(8) (a) Kaplan, J. *J. Chem. Phys.* **1958**, *28*, 278; **1958**, *29*, 462. (b) Alexander, S. *J. Chem. Phys.* **1962**, *37*, 967.
(9) (a) Delpuech, J.-J. *Mol. Phys.* **1968**, *14*, 567. (b) Delpuech, J.-J.; Serratrice, G. *Org. Magn. Reson.* **1972**, *4*, 667.
(10) Anderson, P. W. *J. Phys. Soc. Jpn.* **1954**, *9*, 316.
(11) Kubo, R. *J. Phys. Soc. Jpn.* **1954**, *9*, 935.
(12) Sack, R. A. *Mol. Phys.* **1958**, *1*, 168.
(13) Martin, M. L.; Delpuech, J.-J.; Martin, G. J. "Practical NMR Spectroscopy"; Heyden: London, 1979; pp 441–444.

$$E = \begin{vmatrix} -1 & 0 & 0 & 1 & 0 & 0 \\ 0 & -1 & 0 & 0 & 1 & 0 \\ 0 & 0 & -1 & 0 & 0 & 1 \\ r & 0 & 0 & -r & 0 & 0 \\ 0 & r & 0 & 0 & -r & 0 \\ 0 & 0 & r & 0 & 0 & -r \end{vmatrix} \times k_{inter}$$

All calculations were performed with a Texas Instruments 980A minicomputer equipped with a digital plotter Hewlett-Packard 7210A.

Results

Structure of the Complexes. At room temperature, the proton spectrum of complex **3** consists of (i) a triplet and a doublet at 3.13 and 2.93 ppm, with an intensity ratio of 1:8 (representing the bridging *N*-methyl and terminal *N,N*-dimethyl groups of coordinated NIPA molecules, respectively), and (ii) a multiplet and a triplet at 4.15 and 1.40 ppm, representing the methylene and methyl protons of ethanol. Addition of "free" ethanol to this solution results in two additional groups of signals at low temperatures (<~−30 °C), a methylene quadruplet (overlapping with the lines of NIPA), and a methyl triplet well apart upfield (Figure 2). When the temperature is increased, these lines coalesce with lines ii as the result of a fast intermolecular exchange of free and bound ethanol molecules (see below). Comparing the areas of the bound and free methyl triplets (at low temperatures) allows one to compute the absolute concentration of bound ethanol (from the known concentration of added free ethanol x_0) and in turn to estimate the number of coordinated ethanol molecules in complex **3** (from the known concentration C_0 of the salt). This number is found equal to 1 ± 0.1. The comparison of the areas of the triplet of bound ethanol and of the triplet i of coordinated NIPA allows one in turn to derive the number of coordinated NIPA molecules, i.e., 2 ± 0.2. The composition of the complex is therefore the same in the solution as in the solid salt. Similar conclusions were drawn for the three other complexes. Other pieces of evidence are the absence of perchlorate ions in the first solvation shell of the UO_2^{2+} cation. This is deduced from the absence of IR splitting of the perchlorate absorption line[3,14] at 616 cm^{-1} and from the high value of the molar conductance in nitromethane (160 $cm^2\ \Omega^{-1}\ mol^{-1}$) corresponding to the conductance range (130–180 $cm^2\ \Omega^{-1}\ mol^{-1}$) usually observed for 2:1 electrolytes in this solvent.[15] These observations prove that the salts are completely dissociated in solution and that the formula of the complex uranyl cations is effectively $[UO_2(NIPA)_2X]^{2+}$.

At room temperature, the $^{31}P\{^1H\}$ spectra of complexes **1–4** consist of a single line shifted by ca. 8.0 ppm downfield from the signal of free NIPA at 20.4 ppm. This singlet actually results from the coalescence of an AB-type spectrum (Figure 1) which can be observed at lower temperatures when the intramolecular motion of the NIPA molecules is slow on the NMR time scale. This shows that the insertion of a monodentate ligand is accompanied by the differentiation of the two phosphorus nuclei P_A and P_B in each coordinated NIPA molecule, while both NIPA molecules considered as a whole remain equivalent to each other.

These observations suggest a coordination number of 7 around the central uranium(VI) atom. The seven coordinated oxygen atoms are arranged in a bipyramidal structure where the two apices are the oxygen atoms of the linear O=U=O unit (Figure 3). The pentagonal basis is formed by the four oxygen atoms O_{A1}, O_{B1}, O_{A2}, and O_{B2} from the P=O bonds (P_A,P_B) of each NIPA molecule (further subscripted 1 and 2) and the oxygen atom O_X from the ligand X. This pentagon should possess a symmetry element containing O_X and exchanging the set of O_{A1}, O_{B1} atoms with the O_{A2}, O_{B2} set. This

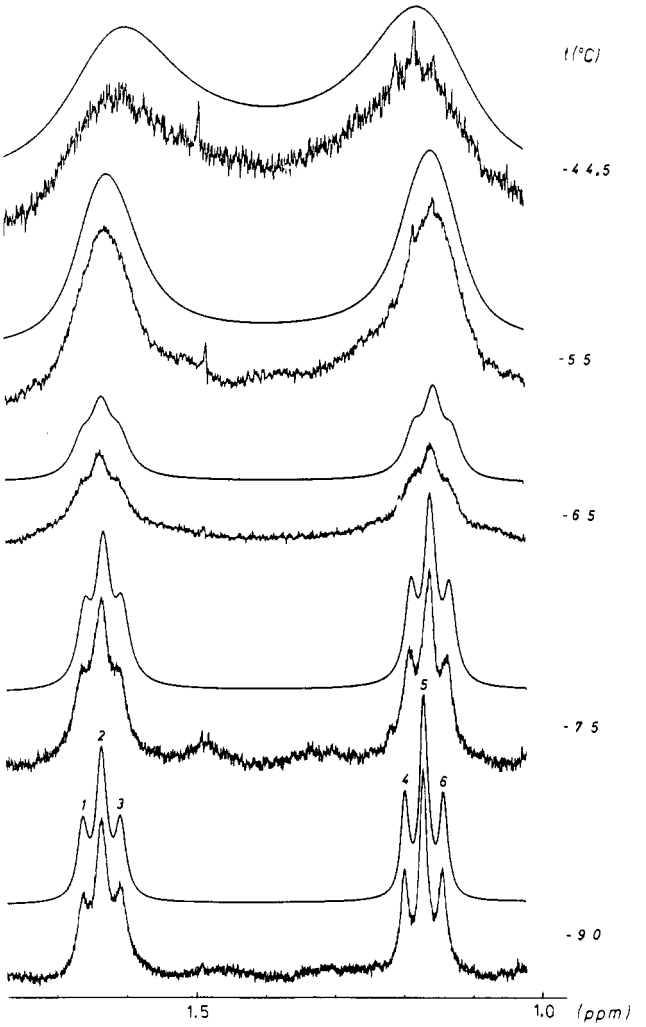

Figure 2. Experimental and calculated best fit ^1H (250 MHz) line shapes (below and above) of a $UO_2(NIPA)_2EtOH^{2+}$ (0.099 M) + ethanol (0.11 M) solution in a 2:1 v/v CH_2Cl_2/CD_3NO_2 mixture, at temperatures of −44.5, −55, −65, −75, and −90 °C (from top to bottom). The coordinated ethanol triplet (lines 1–3) is downfield. Best fit values are k_{inter} = 130, 52, 18, 8.7, and 0 s^{-1}, respectively.

Table I. ^{31}P NMR Parameters of Uranyl Complexes $[UO_2(NIPA)_2X]^{2+}\cdot 2ClO_4^-$ in 0.05–0.10 M Solutions in a 2:1 (v/v) Mixture of Dichloromethane and Nitromethane

complex	T, °C	δ[a]	$\Delta\delta_P$	$^2J_{P-P}$
$[UO_2(NIPA)_2H_2O]^{2+}$	+25	28.5		
	−70	28.94, 29.22	0.28	15.6
$[UO_2(NIPA)_2MeOH]^{2+}$	−70	28.08, 28.98	0.90	15.7
$[UO_2(NIPA)_2EtOH]^{2+}$	+25	28.40		
	−85	28.26, 29.13	0.87	15.7
$[UO_2(NIPA)_2Me_2CO]^{2+}$	−70	28.14, 29.14	1.00	15.6
$[UO_2(NIPA)_2NIPA]^{2+}$	+25	28.40		
	−90	27.09,[b] 29.15	2.06	15.6

[a] δ values are given with respect to an external reference of 85% H_3PO_4 in D_2O. [b] Values for the two doubly bonded NIPA molecules only (see ref 1).

may be achieved by assuming the presence of either (i) a C_2 symmetry axis, in either a *planar configuration of the oxygen pentagon* (Figure 3a)—in which case the planar NIPA molecules are arranged in the equatorial plane and the ligand X along an in-plane C_2 axis,[16] the whole complex belonging to the C_{2v} symmetry point group—or *a puckered configuration*

(14) Airoldi, C.; Gushikem, Y.; Puschel, C. R. *J. Coord. Chem.* **1976**, *6*, 17.
(15) Lannert, K. P.; Joesten, M. D. *Inorg. Chem.* **1968**, *7*, 2048.

(16) In fact, internal rotations are possible along the O–CH_2 and CH_3–CH_2 bonds of ethanol; it may be assumed that the O–CH_2 is directed along the C_2 symmetry axis and that the axial symmetry of the ethanol molecule about the C_2 axis may result from a dynamical average.

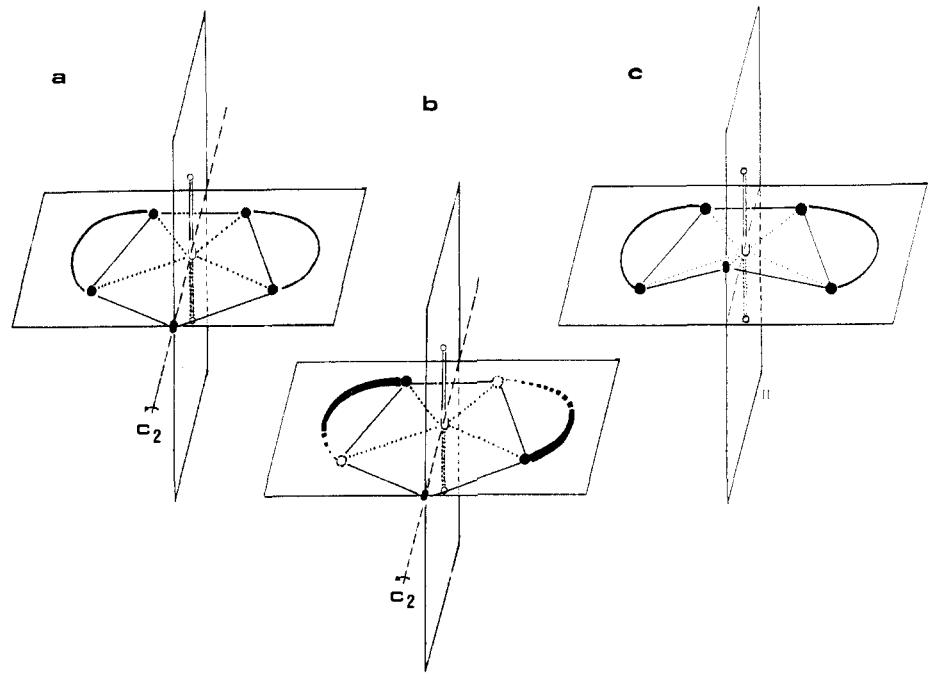

Figure 3. Structures proposed for the complex $[UO_2(NIPA)_2EtOH]^{2+}$ in solution: (a) planar configuration of C_{2v} symmetry; (b) puckered configuration with a C_2 axis; (c) puckered configuration with a vertical plane of symmetry. Phosphoryl groups may be divided in any case into two nonequivalent subsets: $A(P_AO_A)$ and $B(P_BO_B)$.

where the $P{=}O_A$ and $P{=}O_B$ extremities are alternatively displayed above and below the equatorial plane (Figure 3b), or (ii) a *mirror symmetry* about a vertical plane containing the uranyl unit and the ligand X (Figure 3c). Crystallographic studies are in progress to elucidate this point.

As shown in Table I, the chemical shift differences $\Delta\delta_P$ between the P_A and P_B signals decrease as a function of ligand X according to the sequence NIPA >> Me_2CO > EtOH ≃ MeOH >> H_2O. This sequence parallels the order of decreasing size on going from the bulky NIPA molecule (monodentate X ligand in the tris(NIPA) complex $[UO_2(NIPA)_2NIPA]^{2+}$) to the medium-sized alcohols and acetone and finally to the small water molecule. The observed changes in the spectrum would thus be interpreted as a progressive approach of the two bidentate NIPA molecules to a position in which the phosphorus atoms occupy the four corners of a square or rectangle with the uranium atom in its center, thus rendering the ^{31}P nuclei equivalent and reducing the AB spectrum to a single line. It should be further observed that, in the expression $\Delta\delta_P = \delta_{P_A} - \delta_{P_B}$, the term δ_{P_A} has a constant value of 29.12 ± 0.05 ppm. This fact allows us to assign the low-field and high-field ^{31}P resonances, P_A and P_B, to the back and front ends of the coordinated NIPA molecules, respectively (Figure 3). Finally, the chemical shifts of the terminal *N*,*N'*-dimethyl protons of the NIPA molecules should also be different depending on which phosphorus atom (P_A or P_B) they are attached to. This was actually observed in the tris(NIPA) complex where the chemical shift difference was only of 0.02 ppm. With the less bulky ligands X used in the present investigation, the ^1H magnetic inequivalence should be reduced largely (as are the $\Delta\delta_P$ values), resulting in a chemical shift difference within the experimental resolution. Even when the temperature is lowered as far as −90 °C and when a superconducting spectrometer is used, only a weak broadening of the lines could be observed.

It has been shown that uranyl complexes containing two bulky bidentate centrosymmetrical ligands LL may complete their coordination number to 7 or 8 by the insertion of one or two smaller monodentate molecules X. This is the case for the acetylacetonato ligand which gives rise to complexes $UO_2(acac)_2X$, with X = H_2O,[17] NH_3, C_5H_5N,[18] EtOH, or dioxane,[19,20] or for the sulfato or nitrato complexes,[19] which form ions in aqueous solutions such as $UO_2(SO_4)_2(H_2O)_2^{2-}$. An interesting feature of the present study is that the additional neutral monodentate ligand may be in fact a singly bonded bidentate NIPA molecule as in the tris(NIPA) complex. This suggests that with much smaller molecules such as ethanol in complex **3**, some space will be available around the coordination site of ethanol. This possibility will lead to an interesting peculiarity in the kinetics of ligand exchange in the presence of an excess of ethanol, namely, the existence of an outersphere complex accommodating a second ethanol molecule loosely attached to the initial complex ion $[UO_2(NIPA)_2(EtOH)]^{2+}$.

Two types of exchange were in fact observed with the latter complex: an intramolecular exchange of NIPA molecules at temperatures between −30 and +20 °C and an intermolecular exchange of ethanol molecules upon addition of variable amounts of free ethanol, at −75 to −45 °C. The mechanisms and kinetics of these exchanges are examined in the following.

Kinetic Measurements. At temperatures above ca. −50 °C, the resonance lines of the $^{31}P\{^1H\}$ AB patterns of complex **3** are observed to broaden and finally to coalesce into a single line (Figure 1), indicating that some dynamic *intramolecular process* is exchanging sites A and B of each coordinated NIPA molecule. The rate of this internal exchange however was found to depend strongly upon the amount of extra ethanol added to the solution. The values of the NMR rate constant k_{intra} measured for a series of solutions by varying the concentration x_0 of added ethanol and the temperature are reported in Table II. As it is evident from Table II and Figure 5, the exchange rates at a given temperature decrease markedly (by a factor of about 10) when the concentration x_0 is raised from ca. 0.01 to 1.0 mol dm^{-3}. For this reason, it is difficult to measure reliable values for the pure complex (i.e., when x_0 = 0) because of the presence of small quantities of residual

(17) Frasson, E.; Bombieri, G.; Panattoni, C. *Nature (London)* **1964**, *202*, 1325.
(18) (a) Sacconi, L.; Carotti, G.; Paoletti, P. *J. Chem. Soc.* **1958**, 4257. (b) Sacconi, L.; Giannoni, G. *J. Chem. Soc.* **1954**, 2751.
(19) Comyns, A. E.; Gatehouse, B. M.; Wait, E. *J. Chem. Soc.* **1958**, 4655.
(20) Fackler, J. P. *Prog. Inorg. Chem.* **1965**, *7*, 361.

Table II. Experimental Rate Constants k_{intra} (s^{-1}) for the Intramolecular Rearrangement of Coordinated NIPA Molecules in the Complex $[UO_2(NIPA)_2EtOH](ClO_4)_2$ as a Function of the Concentration x_0 of Added Ethanol and of the Temperature[a]

	x_0, mol dm^{-3}					
T, °C	0.011	0.029	0.059	0.102	0.482	1.016
−30.5	10	6.5	*b*	*b*	*b*	*b*
−26.5	15	11	9			
−20.2	28	21	18			
−15.25	43	33	30	16		
−10.0	75	58	43	29	10	
−4.3	110	90	72	57	17	11
+1.1	170	145	110	95	27	18
+5.7	*c*	*c*	145	125	43	26
+10.4			*c*	200	65	38
+14.7				*c*	100	54
+19.0					130	78
+23.5					*c*	105

[a] Conditions: solvent, a 2:1 v/v mixture of dichloromethane and nitromethane; concentration of the complex C_0 = 0.099 mol dm^{-3}; mean accuracy ±10%. [b] Rates beyond the slow exchange limit. [c] Rates beyond the fast exchange rate limit.

Table III. Experimental Rate Constants k_{inter} (s^{-1}) for the Intermolecular Exchange of Ethanol Molecules between the Complex $[UO_2(NIPA)_2EtOH](ClO_4)_2$ and Free Ethanol as a Function of the Concentration x_0 of Added Ethanol and of the Temperature[a]

	x_0, mol dm^{-3}					
T, °C	0.011	0.029	0.059	0.102	0.482	1.016
−75.0	0.9	3.7	5.0	8.7	9.9	9.0
−65.0	2.5	8.0	13.5	18.0	27	30
−55.0	4.5	16.0	32.0	52	57	62
−44.5	16.0	43	75	130	165	150

[a] Same experimental conditions as those reported in Table II.

ethanol due to the procedure employed to prepare the complex. The limiting values k_{ex} of k_{intra} for $x_0 = 0$ consequently result from extrapolation procedures (see Discussion). These values proved to be independent of the concentration C_0 of the complex.

When a solution of the complex containing excess ethanol is chilled to −90 °C, the proton NMR spectrum reveals two groups of signals (Figure 2) corresponding to bound and free ethanol respectively. At higher temperatures an *intermolecular* exchange between the sites for bound and free ethanol molecules is observed. The kinetics of the exchange were measured by using the methyl signals of the alcohol appearing in a region of the spectrum not obscured by other resonances and separated from each other by 0.48 ppm. The NMR exchange rate, k_{inter}, is found to increase sharply (by a factor of about 10) as the concentration x_0 is raised from 0.01 to ca. 0.1 mol dm^{-3} and to remain approximately constant on further addition of ethanol (Table III and Figure 4). The limiting values k of k_{inter} thus obtained proved to be independent from C_0. This is also true for the slope of the tangent at the origin of curves shown in Figure 4 at a given temperature. This suggests kinetic laws of the form

$$k_{intra} = a/(1 + bx_0) \quad (1)$$

$$k_{inter} = cx_0/(1 + dx_0) \quad (2)$$

which were actually to be amended as shown in the Discussion.

Discussion

The Intermolecular Exchange. Among the four mechanisms described by Langford and Gray[21,22] to account for intermolecular ligand substitution, the dissociative (D) or associative (A) mechanisms are not consistent with the rate law of (2). Therefore, we have to consider an interchange (I) mechanism, which may be associative (I_a) or dissociative (I_d). In fact, in the present case where the entering and leaving groups are identical, the distinction between these two variants is impossible according to the criteria of these authors. Such mechanisms assume the initial formation of an outer-sphere complex (OSC) followed by an interchange of ligand molecules X between the first and second coordination spheres according to the general scheme of Eigen and Wilkins[23]

$$[UO_2(NIPA)_2X]^{2+} + X^* \overset{K}{\rightleftharpoons} [UO_2(NIPA)_2X]^{2+}\cdots X^* \overset{k}{\rightleftharpoons} [UO_2(NIPA)_2X^*]^{2+}\cdots X \quad (3)$$

where the asterisk is a topographical distinction only. The corresponding rate constant is given by eq 4 where [X] is the

$$k_{inter} = kK[X]/(1 + K[X]) \quad (4)$$

equilibrium concentration of free ethanol. Equation 4 is identical with the proposed rate law (eq 2) if we replace c and d by kK and K, and x_0 by [X], the concentration of added ethanol not bound in the second coordination sphere (eq 5).

$$[X] = \tfrac{1}{2}[x_0 - C_0 - K^{-1} + ((C_0 - x_0)^2 + (2C_0 + 2x_0 + K^{-1})/K)^{1/2}] \quad (5)$$

Further assumptions in identifying eq 2 with eq 4 are (i) the ethanol molecules in the bulk solvent and in the second coordination sphere of the complex have identical resonance frequencies, (ii) the chemical shifts of the ethanol molecules in the first coordination shell are not altered by the presence of a second ethanol molecule in the second coordination sphere, and (iii) the activity coefficient of free ethanol in the solution

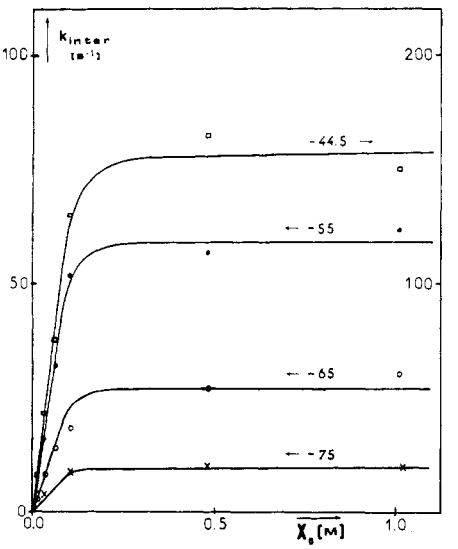

Figure 4. Experimental and best fit curves for the kinetic law $k_{inter} = kK[EtOH]/(1 + K[EtOH])$ (as a function of the concentration of free ethanol) at four temperatures: T = −75 (×), −65 (○), −55 (●), and −44.5 °C (□).

Table IV. Equilibrium Constants K for the Formation of the Outer-Sphere Complex $[UO_2(NIPA)_2EtOH]^{2+}\cdot EtOH^*$ and Rate Constants k for the Interchange of Ethanol Molecules

T, °C	k, s^{-1}	K, dm^3 mol^{-1}	T, °C	k, s^{-1}	K, dm^3 mol^{-1}
−75	9.5	955	−55	59.6	364
−65	27.0	500	−44.5	158	173

(21) Langford, C. H.; Gray, H. B. "Ligand Substitution Processes"; W. A. Benjamin: New York, 1965.

(22) Swaddle, T. W. *Coord. Chem. Rev.* **1974**, *14*, 217.

(23) Eigen, M.; Wilkins, R. G. *Adv. Chem. Ser.* **1965**, *No. 49*, 55.

is equal to unity, while those relative to the free complex and the outersphere complex are equal and cancel out.

After eq 5 is substituted into eq 4, K and k have been adjusted by a nonlinear least-squares fit by using the experimental NMR rate constants (Figure 4). The values of K and k calculated in this way are reported in Table IV. The temperature dependence of K yields the enthalpy and entropy of the outer-sphere formation equilibrium: $\Delta H = -4.8$ kcal mol^{-1} and $\Delta S = -10.7$ cal mol^{-1} K^{-1}. The computed equilibrium constant at room temperature, K(25 °C), is 15.8 dm^3 mol^{-1}. An Arrhenius plot of the rate constants k permitted the evaluation of the activation parameters of the intermolecular exchange reaction; $\Delta H_{inter}^{\ddagger} = 7.6$ kcal mol^{-1}, $\Delta S_{inter}^{\ddagger} = -14.7$ cal mol^{-1} K^{-1}, and of k(25 °C) $= 1.0 \times 10^4$ s^{-1}.

Few examples of an interchange mechanism have been unambiguously demonstrated in the literature[21,22] because, in most cases, eq 4 is reduced to two limiting forms, eq 6 and 7 (depending on whether $K[X] >> $ or $<< 1$) and therefore

$$k_{inter} = k \quad (6)$$

$$k_{inter} = kK[X] \quad (7)$$

cannot be distinguished from the kinetic laws for D or A mechanisms, respectively. Assignments have been made on the basis of structural considerations, solvent effects, and measured volumes of activation.[24,25] A more quantitative procedure, which applies only to unsymmetrical ligand exchanges of the type

$$ML_6 + X \overset{K}{\rightleftharpoons} ML_6 \cdots X \xrightarrow{k} ML_5X + L$$

consists of equating k to the rate constant k_e for the symmetrical solvent exchange $ML_6 + L^* \overset{k_e}{\rightleftharpoons} ML_5L^* + L$. The overall formation rate k_f of the complex ML_5X is then related to k_e and K by an expression analogous to eq 7: $k_f = k_eK$. Independent measurements of k_f and k_e then allow for the computation of the equilibrium constant K.[26-28] For bivalent metal ions reacting with neutral ligands in aqueous solution, values of K found in the literature[29] are in the range of 0.1–0.2 dm^3 mol^{-1}. However, it was shown that the apparently straightforward behavior of aqueous solutions is not general.[26,30] Values of K much higher than expected from the Eigen–Fuoss equations[31,32] of 1.7×10^2–75×10^2 dm^3 mol^{-1} were measured for the substitution of Me_2SO molecules by neutral nitrogen-donor ligands around the aluminum(III) cation in nitromethane solutions.[28] High values of K are also obtained in the present case of an outer-sphere complex involving two identical ethanol molecules as ligands X and L. The driving force for the coordination of a second ethanol molecule could be hydrogen bonding with the ethanol molecule in the first coordination sphere. Evidences supporting this assumption are (i) the enthalpy of formation of the complex (which has an order of magnitude expected for hydrogen bonding) and (ii) the presence of an excess of ethanol in the raw complex salt obtained by precipitation from the reacting solution, with an uncertain stoichiometry ranging between 1 and 2 molecules of ethanol per uranyl cation (the exact stoichiometry of 1 in complex **3** is obtained after the salt is dried on a vacuum line).

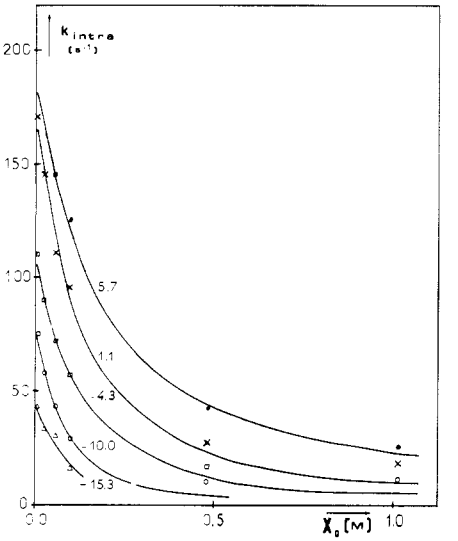

Figure 5. Experimental and best fit curves for the kinetic law $k_{intra} = k_{ex}/(1 + K[EtOH])$ (as a function of the concentration of free ethanol) at five temperatures: $T = -15.3$ (△), −10.0 (○), −4.3 (□), 1.1 (×), and 5.7 °C (●).

Table V. Equilibrium Constants K for the Formation of the Outer-Sphere Complex $[UO_2(NIPA)_2EtOH]^{2+}\cdot EtOH^*$ and Rate Constants k_{ex} for the Intramolecular Rearrangement of NIPA Molecules

T, °C	k_{ex}, s^{-1}	K, dm^3 mol^{-1}	T, °C	k_{ex}, s^{-1}	K, dm^3 mol^{-1}
−15.2	46.1	41.6	−4.3	112.9	18.4
−10.0	78.5	43.8	1.1	175	16.2

The activation parameters are of the same order of magnitude as those observed by Lincoln and co-workers[33,34] for ligand-exchange processes on $UO_2L_5^{2+}$, where L is a monodentate phosphorylated ligand. More precisely, our activation parameters fit reasonably well into a $\Delta H^{\ddagger}$ vs. $\Delta S^{\ddagger}$ linear free energy relationship established in the abovementioned investigations. The authors however could not distinguish between a dissociative and an interchange mechanism, mainly since the assumption of the latter mechanism would have led again to K values much higher than expected from the Fuoss–Eigen equations. The present investigations offer a somewhat unique feature in that parameters k and K may be individually extracted from the experimental data. Our experiments which show the existence of an intermediate outersphere complex are therefore a strong indication in favor of an *interchange mechanism* in all these investigations.

The Intramolecular Exchange. The study of the intramolecular exchange showed that the rate of this exchange decreases when the concentration of added ethanol increases. This suggests that the exchange occurs only on complex **3** and not on the outersphere complex (OSC). The concentration of complex **3** is governed by the equilibrium of the OSC formation (eq 3) and is therefore obtained by multiplying C_0 by the factor $1/(1 + K[X])$.

Consequently, the observed rate constant for the intramolecular rearrangement, k_{intra}, is given by eq 8 where k_{ex} is its

$$k_{intra} = k_{ex}/(1 + K[X]) \quad (8)$$

limiting value in the absence of "free" ethanol when no outersphere complex is present in the solutions. k_{ex} and K were

(24) Meyer, F. K.; Newman, K. E.; Merbach, A. E. *J. Am. Chem. Soc.* **1979**, *101*, 5588.
(25) Ammann, C.; Moore, P.; Merbach, A. E. *Helv. Chim. Acta* **1980**, *63*, 268.
(26) Chattopadhyay, P. K.; Coetzee, J. F. *Anal. Chem.* **1974**, *46*, 2014.
(27) Hoffmann, H.; Janjic, T.; Sperati, R. *Ber. Bunsenges. Phys. Chem.* **1974**, *78*, 223.
(28) Brown, A. J.; Howarth, O. W.; Moore, P.; Parr, W. J. E. *J. Chem. Soc., Dalton Trans.* **1978**, 1776.
(29) Wilkins, R. G. *Acc. Chem. Res.* **1970**, *3*, 408.
(30) Bennetto, H. P.; Caldin, E. F. *J. Chem. Soc. A* **1971**, 2191.
(31) Eigen, M. *Z. Phys. Chem.* **1954**, *1*, 176.
(32) Fuoss, R. M. *J. Am. Chem. Soc.* **1958**, *80*, 5059.
(33) Crea, J.; Digiusto, R.; Lincoln, S. F.; Williams, E. H. *Inorg. Chem.* **1977**, *16*, 2825.
(34) Honan, G. J.; Lincoln, S. F.; Williams, E. H. *J. Soln. Chem.* **1978**, *7*, 443.
(35) Bokolo, K. Thesis, Université de Nancy I, Nancy, France, 1981.

calculated for each temperature by a nonlinear least-squares fit from the experimental NMR data (Figure 5 and Table V). There is some deviation of the experimental points from the theoretical curve (Figure 5) for the higher concentrations of added ethanol, probably because of a decrease of the activity coefficient of free ethanol far below unity when the concentration exceeds ca. 5×10^{-3} mol dm^{-3}. This is not unexpected given the strong self-association of ethanol molecules. This drawback was fortunately circumvented in the above study of intermolecular exchange rates because (i) K was much greater in the temperature range of interest and the concentration of free ethanol was close to 0 for small additions of excess ethanol and (ii) eq 5 was in fact, for large concentrations of added ethanol, reduced to $[X] = x_0$.

As the rate constants k_{ex} are in fact obtained as k_{intra} values extrapolated to 0 concentration of added alcohol, a reasonable accuracy is expected in the adjustment of k_{ex} (ca. ±10%), while the equilibrium constant K is calculated with a large degree of uncertainty (Table V).

For the sake of comparison, values of K have been extrapolated to the same temperatures from the data of Table IV for the intermolecular exchange, yielding $K = 56.3$, 46.7, 38.4, and 32.1 at −15.2, −10, −4.3, and 1.1 °C, respectively. The difference between the two sets of K values are due on one hand to an extrapolation over a wide range of temperature for the latter series and on the other hand to the influence of unknown activity coefficients on the K values of Table V. However, both sets of K values are of the same order of magnitude as expected, showing the validity of the kinetic models used.

From the variations of k_{ex} with temperature, the activation parameters for the internal rearrangement of the NIPA molecules have been determined: $\Delta H_{intra}^{\ddagger} = 10.6$ kcal mol^{-1}, $\Delta S_{intra}^{\ddagger} = -9.4$ cal mol^{-1} K^{-1}, and $k_{ex}(25\ °C) = 9.15 \times 10^2$ s^{-1}.

In order to depict the mechanism for this intramolecular exchange, it seems reasonable to consider that one of the five coordinated oxygen atoms in the pentagonal basis of the bipyramidal structure of Figure 3 is temporarily detached from the uranium center so as to introduce some mobility within the first coordination sphere and thus to promote the rearrangement of the coordinated NIPA molecules. This event may occur in either of two ways:

(a) An ethanol molecule leaves the free complex thus allowing an internal rearrangement of the NIPA molecules via a symmetrical transition state (I). The release of the ethanol

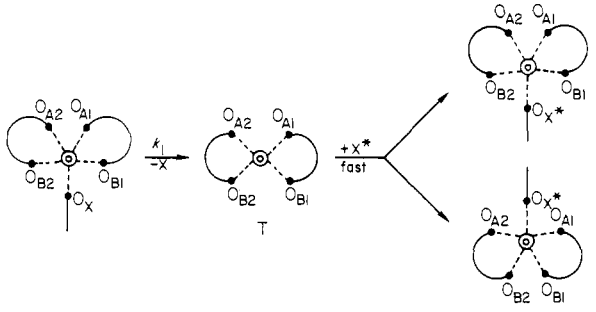

I

molecule is the rate-determining step, followed by a fast return either to the initial configuration of the complex (no NMR exchange) or to its inverted form (accompanied by the NMR exchanges $P_{A_1}P_{B_1} \rightarrow P_{B_1}P_{A_1}$ and $P_{A_2}P_{B_2} \rightarrow P_{B_2}P_{A_2}$ having the same probabilities of $^1/_2$), so that

$$k_{intra} = 0.5k_1/(1 + K[X]) \quad (9)$$

with $k_{ex} = 0.5k_1$ and therefore $k_1(25\ °C) = 1.83 \times 10^3$ s^{-1}, $\Delta H_1^{\ddagger} = 10.6$ kcal mol^{-1}, and $\Delta S_1^{\ddagger} = -8.0$ cal mol^{-1} K^{-1}. Such a mechanism represents a contribution of $k_1/(1 + K[X])$ to the intermolecular exchange rate of ethanol molecules studied above. However, this contribution remains negligibly small within the temperature range studied (−75 to −45 °C) and cannot be detected experimentally. The enthalpy of activation is rather low for such a dissociative mechanism. The entropy of activation is also expected to be positive. The negative value which is actually found may however be accounted for by (i) the association of the ethanol molecule released in the first step with the ethanol molecules from the bulk solution and (ii) the higher symmetry (D_{2d}) of the intermediate I as compared to that of the initial complex (C_2 or C_{2v}).

(b) In a first step, the extremity of one NIPA molecule is detached. The tetracoordinated intermediate returns in a second step to the initial state through the reattachment of the free end of the NIPA molecule. Such a mechanism would correspond to a rate law of the general form given in eq 10.

$$k_{intra} = 0.25k'_1/(1 + K[X]) \quad (10)$$

The factor 0.25 accounts for the fact that only one of the two NIPA molecules detaches one end in the first step and that there is a probability of $^1/_2$ for the free end of NIPA to reenter the complex in such a way that NMR site exchange occurs.

Expression 10 is identical with eq 8 when k_{ex} is substituted for $0.25k'_1$. The kinetic parameters are therefore $k'_1(25\ °C) = 3.66 \times 10^3$ s^{-1}, $\Delta H'^{\ddagger}_1 = 10.6$ kcal mol^{-1}, and $\Delta S'^{\ddagger}_1 = -6.2$ cal mol^{-1} K^{-1}. The rate constant k'_1 is of the expected order of magnitude as compared to the value found for the tris(NIPA complex),[1] $k'_1(25\ °C) = 1.0 \times 10^5$ s^{-1}, where the detachment of the bidentate NIPA ligands is indeed facilitated by the presence of a bulky monodentate ligand (a singly bonded NIPA molecule instead of an ethanol molecule). The negative value of the entropy however does not seem to reflect the apparent increase of ligand mobility in the tetracoordinated intermediate.

No clear-cut evidence allows us to decide between these two mechanisms on the sole basis of the present experiments.

Conclusion. The kinetic studies of the complex $[UO_2(NIPA)_2(EtOH)]^{2+}$ in solution containing excess ethanol have revealed the existence of two interdependent exchange mechanisms: an intermolecular exchange between bound and free ethanol and an intramolecular rearrangement of the NIPA ligands.

The rates of both the exchanges depend on the concentration of added free ethanol. The observed reaction rates are in very good agreement with the formation of an outersphere complex via which the intermolecular exchange takes place. The OSC is in equilibrium with "free" complex (eq 3) on which the intramolecular rearrangement occurs.

The presence of two exchange processes taking place on the same complex species represented a rare occasion for proving the existence of an outer-sphere complex formation which may play an important role in many exchange reactions involving metal complexes.

Acknowledgment. Financial support from the Centre National de la Recherche Scientifique is gratefully acknowledged. All NMR spectra were recorded on spectrometers of the Groupement Régional de Mesures Physiques de l'Académie de Nancy—Metz. We thank M. Diter and Mrs. Eppiger for their technical assistance.

Registry No. **1**, 80126-89-2; **2**, 80126-82-5; **3**, 80126-91-6; **4**, 80105-95-9; $[UO_2(NIPA)_2NIPA](ClO_4)_2$, 80105-97-1.